Theor Chem Acc (2005) 114: 309–317
DOI 10.1007/s00214-005-0692-6

REGULAR ARTICLE

Michal F. Rode · Hans-Joachim Werner

Ab initio study of the O_2 binding in dicopper complexes

Received: 4 July 2005 / Accepted: 22 July 2005 / Published online: 20 September 2005

Abstract The structures and stabilities of $[Cu_2(\mu\text{-}\eta^2\text{:}\eta^2\text{-peroxo})]^{2+}$ (A) and $[Cu_2(\mu\text{-oxo})]^{2+}$ (B) complexes with three NH_3 ligands per copper are investigated using DFT and high-level ab initio methods. These are model systems for active centers in enzymes like hemocyanine and tyrosinase. Previous studies have shown that at the DFT/B3LYP level the peroxo form A is more stable than the μ-oxo form B, while the opposite was found using CASPT2 (Flock M, Pierloot K (1999) J Phys Chem 103:95). At the two computational levels, the energy difference of the isomers differed by more than 30 kcal/mol. In this work this problem is reinvestigated using a localized orbital description and multireference configuration interaction (MRCI) methods. It is found that CASPT2 strongly over-corrects the correlation effect and MRCI predicts structure A to be energetically lower than B, in qualitative agreement with B3LYP and experiment. However, B3LYP seems to stabilize the biradicalic structure A too much, and this effect depends approximately linearly on the amount of exact exchange in the B3LYP density functional. Reducing the amount of exact exchange to 10–15% yields good agreement between MRCI and B3LYP.

Keywords $[Cu_2(\mu\text{-}\eta^2\text{:}\eta^2\text{-peroxo})]^{2+}$ · $[Cu_2(\mu\text{-oxo})]^{2+}$ dicopper-oxygen complexes · oxygen activation · ab initio calculations · DFT · CASPT2 · MRCI

1 Introduction

Dicopper oxygen complexes play an important role in catalysts and enzymes for O_2 activation. They exist in various structures and oxidation states, and have been characterized in the past both experimentally and theoretically (for reviews see Refs. [1–3]). It is believed that oxygen activation is achieved through bonding of the oxygen molecule between the two copper centers, which facilitates redox processes by conversion between different copper oxidation states. One mechanism of reversible O–O bond cleavage, which may take place in enzymes such as hemocyanin, catechol oxidase, and tyrosinase, seems to involve interconversion between two isomers with $[Cu_2(\mu\text{-}\eta^2\text{:}\eta^2\text{-peroxo})]^{2+}$ (A) and $[Cu_2(\mu\text{-oxo})]^{2+}$ (B) cores. The ligands are derivatives of aromatic nitrogen compounds (pyrazole, pyridine, imidazole) [1]. In order to understand the mechanism of these processes in more detail, several previous theoretical studies have attempted to predict the structure and relative energies of such complexes [2, 4–10]. Most studies used density functional theory (DFT) with the B3LYP functional [11]. The validity of this approach has been questioned, however, in an extensive ab initio study of Flock and Pierloot [8] (in the following denoted FP). They used a model system with three NH_3 molecules as ligands at each copper center, and in comparative calculations using B3LYP and CASPT2 (multireference complete active space second-order perturbation theory) they found a huge difference of more than 30 kcal/mol between the predictions of the two methods for the relative stabilities of isomers A and B. At the B3LYP level they found the peroxo structure (A) to be more stable than the μ-oxo (B) by 19.9 kcal/mol, while at the CASPT2 level isomer B was more stable by 12.7 kcal/mol. FP concluded that DFT/B3LYP is not trustworthy for such systems, and that higher level methods like CASPT2 would be needed. However, this contradicts the general experience that B3LYP performs quite well for metal complexes [2], and also that the X-ray structure in hemocyanine [12, 13] corresponds to the peroxo structure, in agreement with the B3LYP prediction. Furthermore, the electronic spectra for hemocyanine and tyrosinase correspond to those of other compounds with $[Cu_2(\mu\text{-}\eta^2\text{:}\eta^2\text{-peroxo}]^{2+}$ core. FP speculated that – in view of the different CASPT2 prediction – the peroxo structure would probably be stabilized by steric or solvent effects.

In this situation, it is a challenging problem of quantum chemistry to find out which of the two methods is actually correct. Unfortunately, the wave functions of both isomers have quite a strong multireference character; in particular, in the peroxo form A, two closed-shell configurations with either

Dedicated to Hermann Stoll on the occasion of his 60th birthday

M.F. Rode · H.-J. Werner (✉)
Institut für Theoretische Chemie, Universität Stuttgart,
Pfaffenwaldring 55, D-70569 Stuttgart, Germany
E-mail: werner@theochem.uni-stuttgart.de

the bonding or antibonding combinations of copper $3d_{xy}$ orbitals have almost the same weight, indicating a biradical character. Thus, single reference methods like CCSD(T) (coupled cluster with single and double excitations and perturbative treatment of triple excitations) cannot be used. Among the variety of multireference methods, CASPT2 is one of the simplest and computationally very efficient. However, the results depend on the choice of the zeroth-order Hamiltonian, and often the CASPT2 method is plagued by intruder state problems. Much more reliable results can be expected by using the variational multireference configuration interaction (MRCI) method [14, 15] or one of its variants like MR-ACPF (averaged coupled pair functional) [16, 17]. Unfortunately, such calculations are much more demanding than CASPT2, and so far MRCI has therefore hardly been applied to larger transition metal complexes. Another disadvantage of MRCI is that it is not size consistent, which leads to errors that grow with system size. However, these errors can be avoided to a large extent by applying the Davidson correction [18–21] or by using the approximately size consistent ACPF method.

In the present work we present large scale MRCI calculations for the same complexes as studied by FP. For comparison, also B3LYP and CASPT2 calculations have been carried out using the same basis sets, which are much larger than the ones used in the previous work. We will show that MRCI predicts that the peroxo structure is lower in energy, in qualitative agreement with B3LYP and experiment, but in strong contrast to CASPT2.

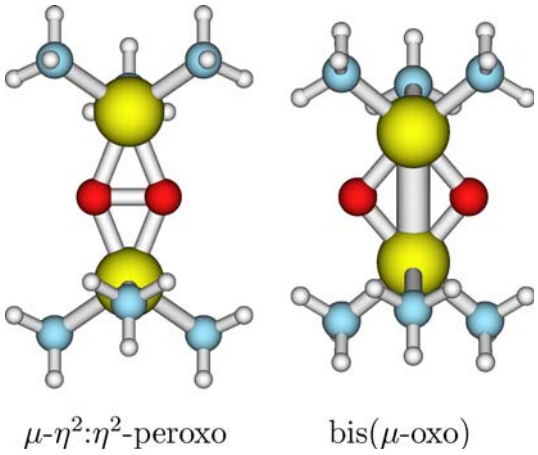

Fig. 1 Optimized CASPT2 structures of the $[Cu_2(\mu\text{-}\eta^2{:}\eta^2\text{-peroxo})]^{2+}$ (**A**) and $[Cu_2(\mu\text{-oxo})]^{2+}$ (**B**) complexes with six NH_3 ligands

Table 1 Optimized bond lengths for isomers A and B (in Å)

	A			B		
Bond	RKS[a]	UKS[a]	CASPT2	RKS[a]	UKS[a]	CASPT2
O–O	1.404	1.468	1.601	2.309	2.309	2.228
Cu–Cu	3.722	3.684	3.486	2.767	2.767	2.864
Cu–N_{eq}	2.059	2.059	2.035	1.980	1.980	1.975
Cu–N_{ax}	2.252	2.251	2.234	2.578	2.578	2.432

[a] Using B3LYP functional [11] and grid target accuracy 10^{-8}. All geometry optimizations were restricted to C_{2h}. The symmetry-broken UKS calculations were done in C_s-symmetry with the xy symmetry plane kept

2 Computational approach

In this work we employed correlation consistent valence double and triple-zeta basis sets, along with an accurate relativistic 10-electron ("small core") pseudopotential for Cu by Stoll and co-workers [22]. The smaller basis consisted of the cc-pVDZ basis sets for Cu [23] and H [24], and the aug-cc-pVDZ basis sets [25] for O and N. In the following, this basis, which comprises 350 contracted functions, will be denoted AVDZ. Single point calculations were also performed with a larger basis, in which the cc-pVTZ basis [23] was used for Cu (this includes two f and one g functions on each copper), the aug-cc-pVTZ basis [25] for N and O, and the cc-pVDZ basis for H. The diffuse functions oxygen were included to allow for a proper representation of the peroxo (O_2^{2-}) character of the O_2 group and of the nitrogen lone pairs of the NH_3 ligands. The larger basis, which included 584 functions, in this paper will be denoted AVTZ. All calculations were performed using the `MOLPRO` package of ab initio programs [26].

The ground state ^1A_g structures A and B were optimized at the spin restricted and unrestricted Kohn–Sham levels (RKS and UKS, respectively) using the B3LYP density functional [11] and the AVDZ basis set. All geometry optimizations were restricted to C_{2h} symmetry. Partial optimizations were also performed at the CASPT2/AVDZ level. In these calculations, which had to be done using numerical gradients, only six parameters were optimized, namely the Cu–Cu and O–O distances as well as the Cu–N distances and Cu–Cu–N bond angles. The NH-bond lengths and all dihedral angles were kept frozen at the UKS/B3LYP values. The resulting structures A and B are shown in Fig. 1. The optimized bond lengths are summarized in Table 1. The orientation of the molecule is the same as in FP. The Cu and O atoms lie on the x- and y axes, respectively (this is relevant for the discussion in Sect. 3). Similar to FP, we also determined approximate reaction paths for isomerization by keeping the O–O distance fixed at a number of values, and optimizing the remaining parameters (in the CASPT2 case, the same partial optimization as described above was performed).

As FP we found a symmetry-broken (spin-contaminated) UKS solution for isomer A, while UKS and RKS converged to the same solution for B. If symmetry adapted RKS orbitals were used as a starting guess in the UKS calculation, the symmetry-broken solution was not reached for structure A. In order to obtain symmetry-broken orbitals, we first performed an RKS calculation for the ^3B_u state, and then rotated the two singly occupied orbitals, which correspond to bonding and anti-bonding combinations of the copper d_{xy}-orbitals, by 45° into each other so that localized d-orbitals were obtained (C_s symmetry was used in the UKS calculations, keeping the xy symmetry plane). Various similar attempts (performed in C_1-symmetry) to obtain a symmetry-broken

solution for structure B were not successful. All calculations converged to the spin-adapted solution.

In the CASPT2 geometry optimizations we used the same active space as FP, namely eight electrons in ten orbitals ($2a_g$, $3a_u$, $2b_u$, $3b_g$). This active space includes the valence MOs resulting from the O($2p_x$) [$O_2(\pi_u, \pi_g)$], O($2p_y$) [$O_2(\sigma_g, \sigma_u)$] and Cu($3d_{xy}$) orbitals, as well as correlating orbitals which have mainly O($3p$) character. The four orbitals resulting from the O($2s$, $2p_z$) AOs are in the inactive space. As demonstrated by FP and confirmed in the present work, correlation of these orbitals has little effect on the relative stabilities of the two isomers, and they are not needed in the active space to obtain qualitatively correct ground-state singlet wavefunctions (they are important, however, for some excited triplet states [8]). Unless otherwise noted, a level shift of 0.3 was used in all CASPT2 calculation to avoid intruder state problems. The standard non-diagonal zeroth-order Hamiltonian was used, and the CASPT2 equations were solved iteratively [27, 28], yielding an orbital-invariant solution. The CASSCF reference functions were optimized using methods as described in Refs. [29, 30].

In order to check the accuracy of the approximations made in the CASPT2 approach, internally contracted MRCI calculations [14, 15] were carried out. Unfortunately, since the MRCI program is limited to treat a maximum of 32 correlated orbitals, full MRCI calculations were not possible for the entire complex. In order to compare MRCI and CASPT2 correlation effects we have therefore performed MRCI and CASPT2 calculations in which only certain orbital subspaces were correlated. In addition, we applied the CIPT2 hybrid method recently developed in our group [31]. In this method the correlated orbital space is divided into two groups, denoted A and C, and the wavefunction is written as $\Psi = \Psi_A + \Psi_C$. Configurations which have exclusively holes in the A-orbital subspace are treated by MRCI, while all remaining excitations are treated by CASPT2. The configuration coefficients are optimized by minimization of the energy functional [31]

$$\begin{aligned} E^{\mathrm{CIPT2}} &= E_{\mathrm{A}}^{\mathrm{CI}} + E_{\mathrm{A}\oplus\mathrm{C}}^{\mathrm{PT2}} - E_{\mathrm{A}}^{\mathrm{PT2}} \\ &= E_{\mathrm{A}}^{\mathrm{CI}} + E_{\mathrm{C}}^{\mathrm{PT2}} + 2\langle\Psi_{\mathrm{C}}|\hat{H}^{(0)}|\Psi_{\mathrm{A}}\rangle \,, \end{aligned} \tag{1}$$

subject to the normalization condition $\langle\Psi^{(0)}|\Psi^{(0)}\rangle = 1$, where $\Psi^{(0)}$ is the reference function which is contained in Ψ_{A}, and $\hat{H}^{(0)}$ is the CASPT2 zeroth-order Hamiltonian. The first term, $E_{\mathrm{A}}^{\mathrm{CI}}$, is the MRCI energy expectation value of Ψ_A, while $E_{\mathrm{C}}^{\mathrm{PT2}}$ is the CASPT2 Hylleraas functional evaluated with Ψ_{C}.

In the present work, the A-space included all active orbitals as well as various subsets of inactive orbitals (see below). If no electrons in the C-space are correlated, the method reduces to MRCI. In order to reduce size consistency errors, the Davidson correction was applied to the MRCI energies and to the MRCI contribution in the CIPT2 as described in Ref. [31]. In the CIPT2 method intruder state problems are absent and no level shift was applied. For comparison, some calculations were also performed with the MR-ACPF method [16, 17].

Normally, the optimized inactive CASSCF orbitals are transformed to pseudo-canonical form by block-diagonalizing an effective Fock operator. In the present case, this leads to delocalized orbitals which are strongly mixed with contributions from all atoms. These orbitals are unsuitable for a meaningful definition of independent orbital subspaces. A nice separation is possible, however, using Pipek–Mezey localization [32], as implemented in `MOLPRO`. The Cu $3s$, $3p$ and O, N $1s$ orbitals were not correlated and left in the canonical form. If C_{2h} symmetry is used in the calculation, the procedure yields symmetry adapted linear combinations of five different groups of localized orbitals: O($2s$), O($2p_z$), Cu($3d$), nitrogen lone pairs, and N–H bonding orbitals. This makes it possible to keep certain well defined orbital subsets either entirely uncorrelated or to select them as C-space in the CIPT2 approach.

In order to reduce the computational effort of the MRCI and CIPT2 calculations, the active space was reduced in the reference functions by one weakly occupied orbital in each symmetry, yielding a CAS(8,6) reference space. The orbitals were always taken from the CASSCF(8,10) (natural orbitals were used in the active space, and the orbitals with the lowest occupation numbers were omitted in the CAS(8,6) reference functions). Test calculations show that such reductions of the reference space have a rather small effect on the relative energies (see Table 3). The CASPT2 energy differences change by about 1.5 kcal/mol. Surprisingly, it was found that the effect is somewhat larger if the NH bond electrons are not correlated. Some calculations were therefore also performed using CAS(8,7) reference functions, in which the weakly occupied a_g orbital was included. Unfortunately, this strongly increases the cost of the MRCI, and using this larger space was therefore not possible in all calculations.

3 Results and discussion

Figure 2 shows typical symmetry-adapted localized inactive orbitals. One can clearly distinguish copper d-orbitals, nitrogen lone pairs, and N–H bond orbitals. The oxygen $2s$, $2p_z$ orbitals are similarly well localized and not shown. Only the totally symmetric combinations are plotted, but the functions for other symmetries look very similar, apart from the signs. The form of the active orbitals has already been discussed by FP and other authors, and therefore they are not reproduced here again.

Table 2 defines the orbital subspaces which are distinguished in the subsequent calculations. The results of calculations using various different A- and C-subspaces are presented in Table 3 for the AVDZ basis sets. Even though this basis is too small to obtain fully quantitative results, we believe that the qualitative observations would be the same for larger basis sets. The calculations have been performed at the optimized CASPT2 structures.

The first two columns of Table 3 show CASPT2 and MRCI calculations in which only the electrons in the A-space were correlated. This allows for a direct comparison of the two methods using exactly the same configuration spaces. The results of CIPT2 calculations are listed in the last column of Table 3. In this case, the excitations arising solely

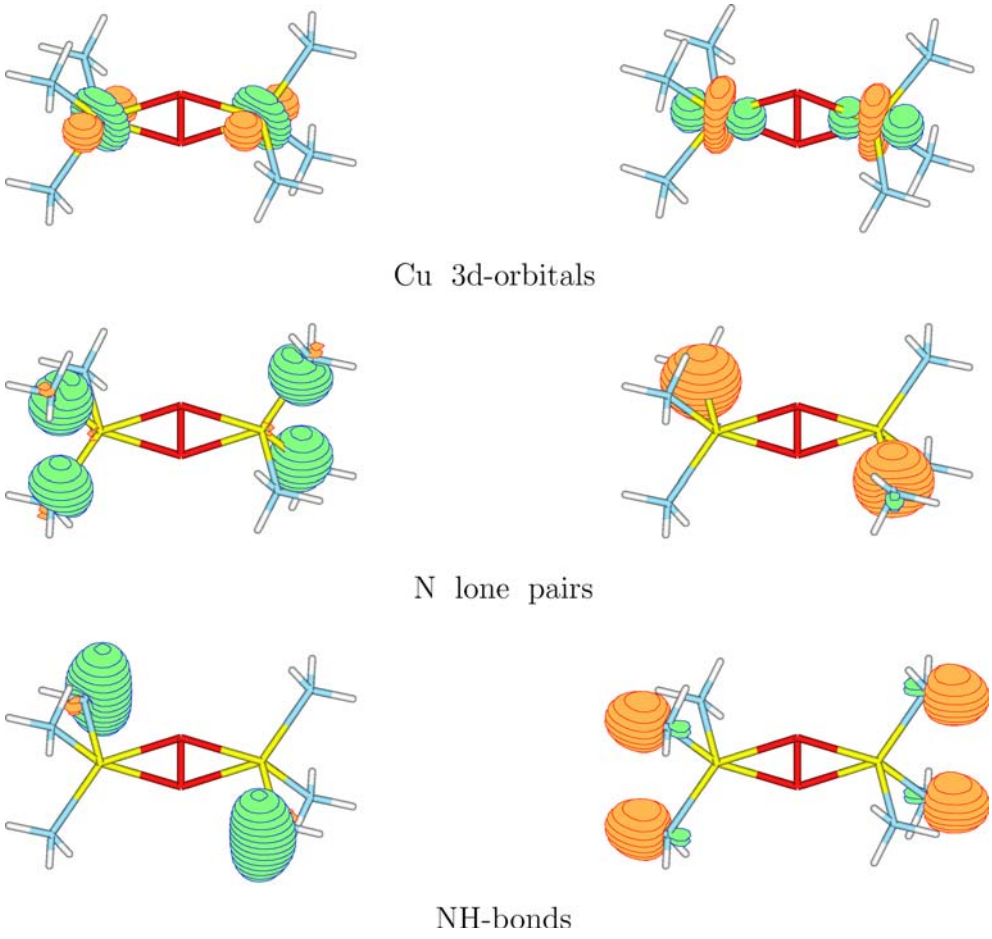

Fig. 2 Symmetry-adapted localized inactive orbitals

Table 2 Localized orbital subspaces

Space	Orbitals
Core	O(1s), N(1s), Cu(3s, 3p)
act	O(2p_x, 2p_y, 3p_x, 3p_y), Cu(3d_{xy})
NH	N–H bond orbitals
N	N(lone pairs)
O	O(2s, 2p_z)
Cu	Cu(3d_{z^2}, 3$d_{x^2-y^2}$, 3d_{xz}, 3d_{yz})

from A-space orbitals are treated by MRCI, similar to the calculations in the second column. In addition, all remaining configurations involving excitations from the C-space are also included and treated by CASPT2, as described in Sect. 2.

In the first calculation, in which the A-space is denoted *act*, only the eight active electrons were correlated in the CASPT2 and MRCI. The effect is very small and the energy differences $\Delta E_{AB} = E(B) - E(A)$ remain close to the CASSCF(8,10) value, which amounts to 23.90 kcal/mol. The result of the CIPT2 calculation is close to the full CASPT2 result. Consistent with the MRCI result, the variational treatment of excitations from the active space leads to a slightly less negative energy difference.

Table 3 Energy differences $\Delta E_{AB} = E(B) - E(A)$ (in kcal/mol) computed with different methods and orbital subspaces[a]

Ref.	A-Space	CASPT2[b]	MRCI+Q[a,b]	CIPT2+Q[c]
(8,10)	Reference		23.90	
(8,6)	Reference		25.11	
(8,10)	act	23.45	24.16	−7.53
(8,6)	act	21.67	24.24	−7.29
(8,6)	act,Cu	5.75	15.32	0.10
(8,6)	act,Cu,O	3.70	16.97	4.11
(8,6)	act,Cu,N	0.34	12.00	2.57
(8,6)	act,Cu,N,O	−3.83	12.42	7.45
(8,6)	act,Cu,N,O,Cu(3p)[d]	−5.54	12.48	
(8,6)	act,Cu,N,O,NH(a_g)	−4.86	12.27	
(8,6)	act,Cu,N,O,NH(a_u)	−5.17	11.85	
(8,6)	act,Cu,N,O,NH(b_u)	−6.10	11.04	
(8,6)	act,Cu,N,O,NH(b_g)	−5.24	11.76	
(8,6)	full[f]	−8.85	(10.0)[e]	
(8,10)	full[f]	−7.37		

[a] Basis AVDZ; the O(1s), N(1s), and Cu(3s, 3p) electrons were not correlated
[b] C-space treated as core (not correlated)
[c] C-space treated by CASPT2, see text
[d] Including Cu(3p) correlation, using the cc-pCVDZ basis set [23] for Cu
[e] Estimated value using increments for NH correlation
[f] Without correlation of the Cu(3s,3p) electrons

The situation changes drastically if the eight additional copper d-orbitals are included in the correlation treatment. At the CASPT2 level, this stabilizes structure B by as much as 16 kcal/mol relative to A. On first sight this is surprising, since in structure B, where copper is in oxidation state Cu(III), there are formally less electrons in the d-shell than in structure A, which corresponds to Cu(II). Nevertheless, the correlation energy is larger in B than in A. A more detailed analysis shows that the correlation energy contribution of the double excitations into the external space, which describe dynamical correlation effects, is indeed smaller in B than in A. However, the opposite is true for the semi-internal excitations which describe polarization and relaxation effects, and these are more important in B than in A. It appears that these subtle effects are rather strongly overestimated in the CASPT2 method. The MRCI+Q lowers structure B only by about 9 kcal/mol, i.e., 7 kcal/mol less than CASPT2. This trend continues as more orbitals are included in the A-space, and the difference between CASPT2 and MRCI+Q increases in each step. If only the NH bond orbitals are treated as core, CASPT2 over-stabilizes B by more than 16 kcal/mol relative to MRCI+Q. The CIPT2 results in the last column of Table 2 are consistent with these results. In each case, the difference between MRCI and CIPT2 corresponds approximately to the difference between the CASPT2 results for the corresponding orbital space and the full space. For example, in the calculation with orbital groups Cu,O,N in the A-space, the CASPT2 in the first column does not include the correlation effect of the NH bonds. Comparison with the full CASPT2 shows that this amounts to about 5 kcal/mol. Correspondingly, the difference between MRCI+Q and CIPT2+Q is also 5 kcal/mol. Due to the coupling of MRCI and CASPT2 in the CIPT2 method, the MRCI and CASPT2 contributions are not exactly additive, however.

Unfortunately, we were not able to perform MRCI calculations for the whole system, since our program is restricted to a maximum of 32 correlated orbitals. In order to investigate the effect of correlating the NH bonds, it was only possible to include the symmetry-adapted NH orbitals for one irreducible representation at a time, and to use an incremental scheme [33–36] to estimate the total effect. The sum of the CASPT2 contributions for all NH-bonds amounts to −6.05 kcal/mol, which can be compared to the value of −5.02 kcal/mol obtained from the full calculation. The difference arises from the neglect of correlations between the groups of NH orbitals. At the MRCI+Q level, correlation of the NH bond electrons has a smaller effect. In this case the sum of the contributions amounts to −2.75 kcal/mol. Taking into account that this value probably slightly overestimates the contribution, we arrive at a final estimate of 10 kcal/mol for the MRCI+Q energy difference. This value lies between the UKS/B3LYP and RKS/B3LYP results (16.69 kcal/mol and 6.14 kcal/mol, respectively), while the corresponding CASPT2(8,7) (−8.85 kcal/mol) gives qualitatively a wrong prediction of the relative stabilities of the two isomers.

The effect of correlating the copper 3p electrons has been tested using a recently developed cc-pCVDZ basis set [23]. This basis cannot be expected to give quantitative results, but it can at least indicate whether a significant effect occurs. At the MRCI+Q level (without the NH bond electrons being correlated) the effect is found to be negligible, while at the corresponding CASPT2 level structure B is further stabilized by 1.7 kcal/mol.

In order to check that the overshooting of CASPT2 is not due to a hidden intruder state problem, we tested the dependency of the CASPT2 results on the level shift, which was 0.3 hartree in all calculations discussed above. The dependence of the energy difference on the level shift is shown in Fig. 3. Using the AVDZ basis set and the CAS(8,6) reference functions no convergence problems were encountered even with zero shift. As expected, the correlation effect gets smoothly smaller with increasing level shift. Thus, the overshooting of the CASPT2 correlation contribution is even larger without a shift, but there is no singularity. We also tested the g_1 zeroth-order Hamiltonian of Andersson [37], but in this case intruder problems occured even with a level shift of 0.4 hartree.

The effect of increasing the basis set on the predicted energy differences is shown in Table 4 for DFT, CASPT2 and MRCI, and MR-ACPF. For comparison, the results of FP are listed in the last column. It is found that the basis set effect is rather small at the DFT and CASSCF levels, i.e., the AVDZ basis appears to be flexible enough to describe well the occupied orbital space. The effect is significantly larger at the CASPT2(8,10) level; using the AVTZ basis the energy difference becomes about 3 kcal/mol more negative; for CASPT2(8,6) the effect is even somewhat larger. However, at the MRCI+Q and MR-ACPF levels (without correlation of the NH bond electrons), the basis set effect is less than 1 kcal/mol. This indicates that the overshooting of the

Table 4 Dependence of the energy difference ΔE_{AB} (in kcal/mol) on the basis set

Method	AVDZ	AVTZ	FP [8]
UKS/B-LYP[a]	2.71	0.91	
RKS/B-LYP[a]	2.81	0.80	
UKS/B3LYP[a]	16.69	15.29	19.9[d]
RKS/B3LYP[a]	6.14	4.08	14.4[d]
UKS/BH-LYP[a]	54.89	53.25	
RKS/BH-LYP[a]	6.58	3.81	
CASSCF(8,10)[b]	23.90	23.44	23.2[e]
MRCI+Q(8,6)[b,c]	12.42	11.61	
MR-ACPF(8,6)[b,c]	10.62	9.35	
CASPT2(8,6)[b]	−8.85	−12.21	
CASPT2(8,10)[b]	−7.37	−10.24	−11.5[e]

[a] Computed at the optimized structures of the corresponding method and the AVDZ basis set. All DFT values were obtained with the MOLPRO default grid (target accuracy 10^{-6})
[b] Computed at the optimized CASPT2(8,10)/AVDZ structures
[c] NH bond electrons were not correlated in MRCI and ACPF
[d] 6-31G* basis for H,N,O; double ζ basis, augmented by diffuse p, d and f-functions for Cu, see Ref. [8]
[e] All-electron calculations using the ANO-S DZP basis and including a first-order relativistic correction

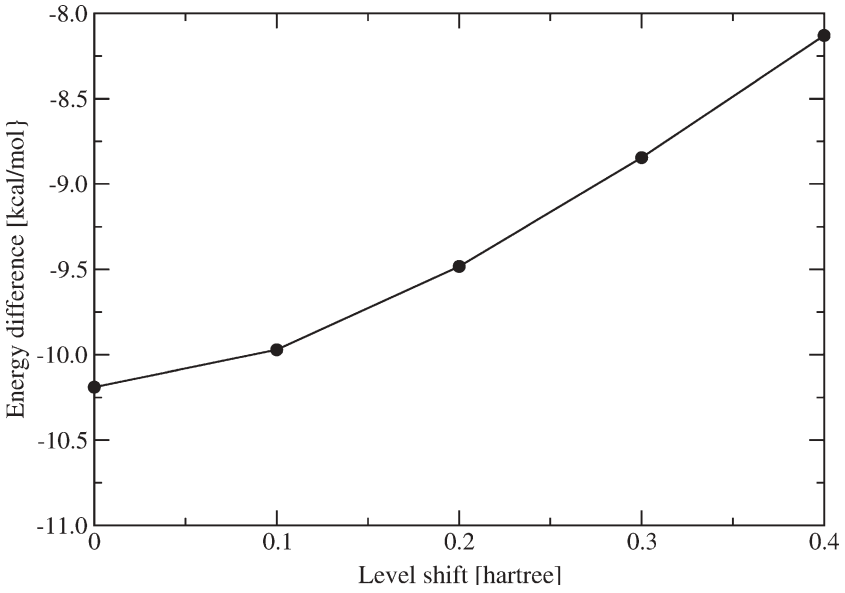

Fig. 3 Dependence of the CASPT2(8,10) energy difference E(B)−E(A) (in kcal/mol) on the level shift using the (8,6) reference space

CASPT2 method increases with increasing basis set size, as it is rather typical for perturbational approaches. It is found that MR-ACPF leads to a somewhat smaller energy difference than MRCI+Q. Since the effect of the size consistency correction is negative, ACPF gives a larger size consistency correction, but presently it cannot be decided which method is more accurate. The disadvantage of MR-ACPF is that convergence is much slower than in MRCI, and therefore the computational cost is significantly higher.

Our CASSCF and CASPT2 results are in good agreement with those of FP, who performed all-electron calculations using basis sets of double ζ quality. In their CASPT2 results a relativistic correction was included, which was computed by first-order perturbation theory using the Darwin and mass-velocity terms. In our calculations, relativistic effects are accounted for in the pseudopotential. Significant differences are found, however, at the RKS and UKS/B3LYP levels. Partly, these are due to relativistic effects, which were not taken into account in the DFT calculations of FP, and which reduce the energy difference by about 4 kcal/mol. If this is taken into account, the UKS/B3LYP results are in reasonable agreement. However, in our calculations the difference between RKS and UKS is much bigger than in the work of FP. Possibly, this is due to the rather small basis set used in the latter work.

Table 4 also demonstrates the effect of the chosen density functional on the computed energy differences. Apart from B3LYP, we have tested two different functionals, namely B-LYP without exact exchange, and BH-LYP with 50% exact exchange included. It is found that the amount of exact exchange has a drastic effect on the results: while with B-LYP the energy difference of both isomers is small, structure A is dramatically over-stabilized using BH-LYP, which includes 50% exact exchange and 50% of the Becke exchange functional [38]. It appears that B3LYP (20% exact exchange) is a reasonable compromise, but this seems to be rather fortuitous.

Recently, Reiher et al. [39] have reported that low-spin/high-spin splittings in Fe(II) transition-metal complexes are also heavily influenced by the amount of exact exchange in the density functional used. They found that the computed energy splittings depend almost linearly on the amount of exact exchange. In order to improve agreement with experiment, they suggested to reduce the amount of exact exchange from 20% in B3LYP to 15%. This value was considered as an upper bound and chosen to change the B3LYP functional as little as possible; the optimum region was found between 8 and 16%. Inspired by this work, and in view of the above findings, we have computed the energy difference as a function of the c_3 coefficient in the B3LYP functional, which determines the amount of exact exchange. The calculations were performed at the UKS/B3LYP geometries without reoptimization, since by comparison of B-LYP, B3LYP, and BH-LYP results it was found that the functional does not have a big effect on the structures, and that the energy differences are not sensitive to the reoptimization. Amazingly, we also find an almost linear dependence of the energy difference on c_3 (see Fig. 4), and using values between 0.1 and 0.15 yields results which are close to the MRCI+Q value. At the same time, when the fraction of exact exchange is reduced, the expectation value of $\hat{S}^2$ also decreases, i.e., the amount of triplet contamination reduces (the expectation values of $\hat{S}^2$ are 0.96, 0.73, and 0.03 for BH-LYP, B3LYP, and B-LYP at the corresponding optimized structures A). This is consistent with the fact that exact exchange stabilizes the high-spin states relative to the singlet ground state. Thus, by an appropriate choice of c_3, the functional can be tuned to better reproduce high level calculations, and this might be useful for future calculations with larger and more realistic ligands. However, more experience is certainly needed to decide if the reduction of exact

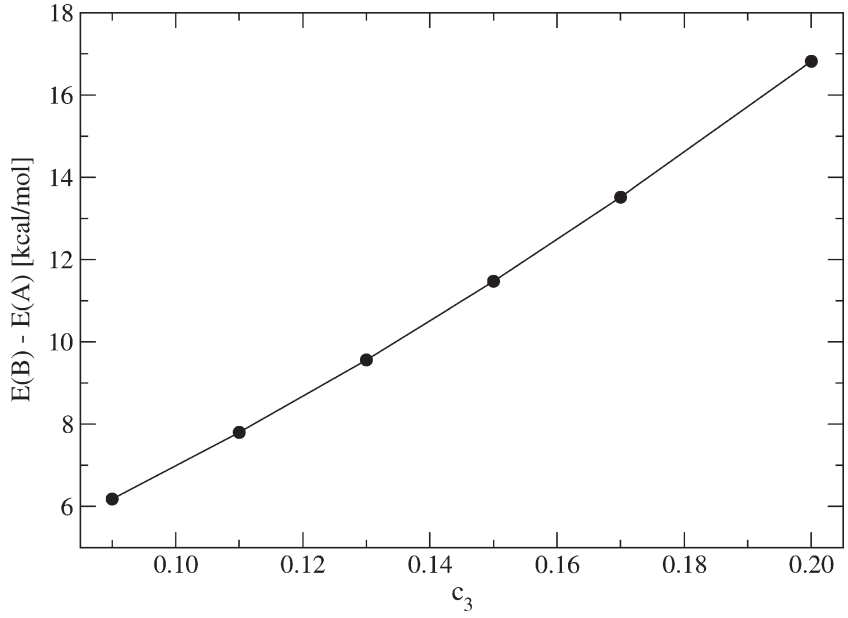

Fig. 4 Effect of the amount of exact exchange in the B3LYP functional on the computed UKS/AVDZ energy difference

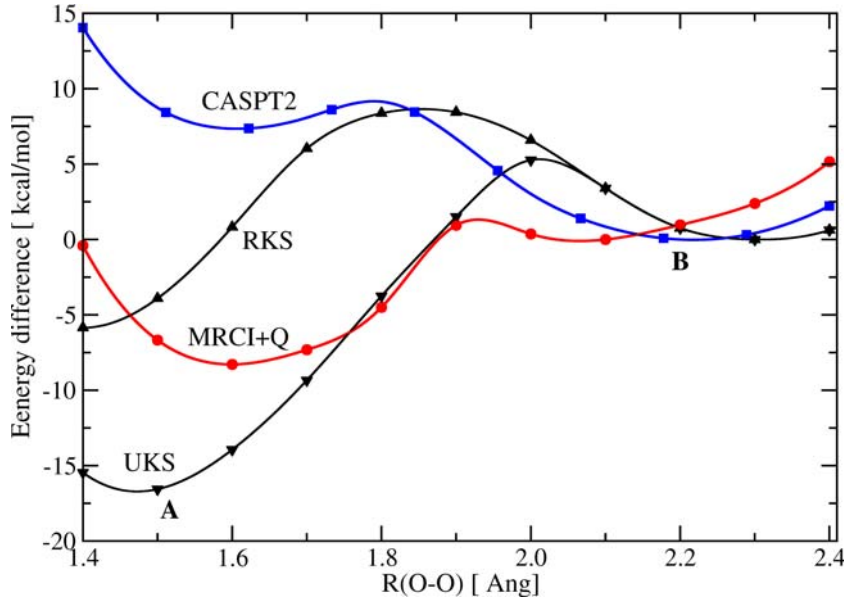

Fig. 5 Isomerization energy profiles using different methods (see text)

exchange leads in general to better results for transition metal complexes.

Finally, in Fig. 5 the energy profiles along the isomerization reaction coordinate are presented. These calculations have been done with the AVDZ basis, and the minimum energies at structure B have been taken as zero points. Low barriers are found at all levels of calculation. In the UKS/B3LYP case, the barrier is near the place where symmetry breaking occurs. On the side towards B, the UKS wavefunction is spin- and symmetry-adapted, while on the side towards A the symmetry-broken solution is obtained. Consequently, between the barrier and B the RKS and UKS potentials are identical. As in the calculations of FP, the CASPT2 barrier is shifted to a shorter O–O distance as compared to the UKS and RKS ones. The CASPT2 minimum for structure A is somewhat more pronounced than in FP, which could be due to the larger basis set used in the present calculations. Also, in our work the CASPT2 geometries were more extensively optimized (in the work of FP, only the Cu–Cu distance was re-optimized for each O–O distance, while in the present work the Cu–N bond lengths and bond angles were also optimized). The MRCI calculations have been performed with CAS(8,7) reference space, in which the orbital $19a_g$ has been included. It was found that this has a non-negligible effect on the relative

energies, and inclusion of this orbital in the reference stabilizes B relative to A by about 3 kcal/mol. Nevertheless, the MRCI+Q curve does not look as smooth as the others, which can be attributed to the fact that the geometry was taken from the CASPT2(8,10) calculation. Due to high expense, we were not able to reoptimize the geometries for MRCI. However, we have compared the MRCI+Q energies at the optimized RKS, UKS, and CASPT2 minima and found for both A and B that the MRCI+Q energy is lowest at the CASPT2 structures, and highest at the RKS ones. Thus, the CASPT2 structures seem closest to the MRCI+Q ones. The MRCI+Q potential along the optimized CASPT2 reaction path has a very low barrier. The minimum for structure A is at about the same position as in CASPT2, while the minimum for B is rather shallow and shifted to a shorter O–O distance. In these MRCI calculations, the NH bond electrons were not correlated; as shown earlier, inclusion of all electrons would stabilize structure B relative to A by about 2 kcal/mol. A further stabilization of about 2 kcal/mol would result if MR-ACPF was used instead of MRCI+Q. And finally improvements of the basis set also stabilize B by 1–2 kcal/mol. Taking all effects together, one arrives at an estimate of 6–8 kcal/mol for the energy difference between structures B and A.

It should be noted that the CASPT2 and MRCI+Q O–O distances of about 1.6 Å for the peroxo form A are significantly longer than the O–O distances in enzymes (about 1.41 Å). Furthermore, the Cu–Cu distance seems to be too short in A and too long in B. The reason for these deviations is still unknown. Possibly, correlation of the $3p$ electrons in Cu, which has neither been taken into account in the present work nor by FP, would have an effect on the structures. Previous work for the Cr_2-dimer has demonstrated that the $3p$-correlation shortens the bond distance by about 0.1 Å. [31]. Unfortunately, this effect was also not correctly described by CASPT2 [31], and therefore very extensive MRCI calculations, would be necessary to clarify this question.

4 Conclusions

MRCI+Q and MR-ACPF calculations with large basis sets show that for the model complex studied in this work, the $[Cu_2(\mu\text{-}\eta^2\text{:}\eta^2\text{-peroxo})]^{2+}$ form is more stable by 6–8 kcal/mol than the $[Cu_2(\mu\text{-oxo})]^{2+}$ form. This is in qualitative agreement with the experimental finding that the peroxo form occurs in enzymes, and also with the predictions of UKS/B3LYP calculations. However, the latter method seems to overstabilize the peroxo form by almost a factor of two. It has been found that the predicted B3LYP energy difference depends approximately linearly on the amount of exact exchange in the functional, and reducing this from 20% to 10–15%, as recently proposed by Reiher et al. [39], gives much better agreement between MRCI+Q and B3LYP. In contrast to B3LYP, MRCI, and MR-ACPF, CASPT2 favors the μ-oxo form by more than 12 kcal/mol. Since there is no theoretical or experimental reason to trust CASPT2 more than MRCI or MR-ACPF, it must be concluded that the CASPT2 method is not useful for predicting energy differences of transition metal complexes in which the metals are in different oxidation states. Another similar dramatic failure of CASPT2 was recently reported in a study of various isomers of S_3O, which have a different amount of biradical character [40]. As in the present case, CASPT2 predicted the relative energies in the wrong order. Compared to MRCI+Q and CCSD(T) calculations, the CASPT2 energy differences were in error by more than 40 kcal/mol.

The current work does not resolve the discrepancy between the computed CASPT2/MRCI+Q and experimental O–O and Cu–Cu bond distances in the complexes. Even though a direct comparison of experimental data with the current very simplified model system is questionable, further work is desirable to investigate whether core correlation, larger basis sets, and geometry optimization at the MRCI+Q level have an effect on the structures. Preliminary results indicate that the inclusion of Cu($3p$) correlation has a small effect on the relative energy computed at the CASPT2 structures, but no geometry optimization including the $3p$ correlation has been carried out so far. The main conclusion of this work, namely that CASPT2 predicts quantitatively and qualitatively wrong energetics for this system, is unaffected by these questions.

Acknowledgements This work has been supported by the Deutsche Forschungsgemeinschaft and the Fonds der Chemischen Industrie. We thank Prof. Kirk Peterson for providing the correlation consistent basis sets for copper prior to publication.

References

1. Micica LM, Ottenwaelder X, Stack TDP (2004) Chem Rev 104:1013
2. Siegbahn PEM (2003) Faraday Discuss. 124:289
3. Siegbahn PEM, Blomberg MRA (1999) Ann Rev Phys Chem 50:221
4. Bernadi F, Bottoni A, Casadia R, Fariselli P, Rigo A (1996) Inorg Chem 35:5207
5. Cramer CJ, Smith BA, Tolman WB (1996) J Am Chem Soc 118:11283
6. Bérces A (1997) Int J Quantum Chem 65:1077
7. Bérces A (1997) Inorg Chem 36:4831
8. Flock M, Pierloot K (1999) J Phys Chem A 103:95
9. Lam BMT, Halfen JA Jr, Young VG, Hagadorn JR, Holland PL, LLedos A, Cucurull-Sanchez L, Novoda JJ, Alvarez S, Tolman WB (2000) Inorg Chem 39:4059
10. Metz M, Solomon EI (2001) J Am Chem Soc 123:4938
11. Becke AD (1993) J Chem Phys 98:5648
12. Volbeda A, Hol WG (1989) J Mol Biol 209:249
13. Magnus KA, Hazes B, Ton-That H, Bonaventura C, Bonaventura J, Hol WG (1994) J Proteins 19:302
14. Werner H-J, Knowles PJ (1988) J Chem Phys 89:5803
15. Knowles PJ, Werner H-J (1988) Chem Phys Lett 145:514
16. Gdanitz RJ, Ahlrichs R (1988) Chem Phys Lett 143:413
17. Werner H-J, Knowles PJ (1990) Theor Chim Acta 78:175
18. Langhoff SR, Davidson ER (1974) Int J Quantum Chem 8:61
19. Davidson ER (1974) In: Daudel R, Pullman B (eds) The world of quantum chemistry, Reidel, Dordrecht
20. Taylor PR (1992) Accurate calculations and calibration. In: Roos BO (eds) Lecture notes in quantum chemistry, vol 58. Springer, Berlin Heidelberg New York

21. Knowles PJ, Schütz M, Werner H-J (2000) Ab initio methods for electronic correlation in molecules. In: Johannes Grotendorst (eds) Modern methods and algorithms of quantum chemistry, vol 3. NIC-Directors
22. Figgen D, Rauhut G, Dolg M, Stoll H (2005) Chem Phys 311:227
23. Peterson KA, Puzzarini C (2005) Theor Chem Acc (in press)
24. Dunning TH Jr (1989) J Chem Phys 90:1007 (currently online, DOI: 10.1007/s00214-005-0689-9)
25. Kendall RA, Dunning TH Jr, Harrison RH (1992) J Chem Phys 96:6796
26. MOLPRO is a package of ab initio programs designed by Werner H-J, Knowles PJ, written with contributions from Amos RD, Bernhardsson A, Berning A, Celani P, Cooper DL, Deegan MJO, Dobbyn AJ, Eckert F, Hampel C, Hetzer G, Knowles PJ, Korona T, Lindh R, Lloyd AW, McNicholas SJ, Manby FR, Meyer W, Mura ME, Nicklass A, Palmieri P, Pitzer R, Rauhut G, Schütz M, Schumann U, Stoll H, Stone AJ, Tarroni R, Thorsteinsson T, Werner H-J, see http://www.molpro.net
27. Werner H-J (1996) Mol Phys 89:645
28. Celani P, Werner H-J (2000) J Chem Phys 112:5546
29. Werner H-J, Knowles PJ (1985) J Chem Phys 82:5053
30. Knowles PJ, Werner H-J (1985) Chem Phys Lett 115:259
31. Celani P, Stoll H, Werner H-J (1004) Mol Phys 102:2369
32. Pipek J, Mezey PG (1989) J Chem Phys 90:4916
33. Stoll H (1992) Phys Rev B 46:6700
34. Stoll H (1992) J Chem Phys 97:8449
35. Stoll H (1992) Chem Phys Lett 191:548
36. Kalvoda S, Paulus B, Dolg M, Stoll H, Werner H-J (2001) Phys Chem Chem Phys 3:514
37. Andersson K (1995) Theor Chim Acta 91:31
38. Becke AD (1988) Phys Rev A 38:3098
39. Reiher M, Salomon O, Hess BA (2001) Theor Chem Acc 107:48
40. Wong MW, Steudel R (2005) Chem Comm 29:3712